International Journal of
Molecular Sciences

MDPI

Article

Evidence for Dual Activation of $I_{K(M)}$ and $I_{K(Ca)}$ Caused by QO-58 (5-(2,6-Dichloro-5-fluoropyridin-3-yl)-3-phenyl-2-(trifluoromethyl)-1H-pyrazolol[1,5-a]pyrimidin-7-one)

Chao-Liang Wu [1,†], Poyuan Fu [2,†], Hsin-Yen Cho [3], Tzu-Hsien Chuang [3] and Sheng-Nan Wu [3,4,*]

[1] Department of Medical Research, Ditmanson Medical Foundation Chia-Yi Christian Hospital, Chiayi 60002, Taiwan; wumolbio@mail.ncku.edu.tw
[2] Department of Ophthalmology, Ditmanson Medical Foundation Chia-Yi Christian Hospital, Chiayi 60002, Taiwan; 07141@cych.org.tw
[3] Department of Physiology, National Cheng Kung University Medical College, Tainan 70101, Taiwan; s36094083@gs.ncku.edu.tw (H.-Y.C.); s36091051@gs.ncku.edu.tw (T.-H.C.)
[4] Institute of Basic Medical Sciences, National Cheng Kung University Medical College, Tainan 70101, Taiwan
* Correspondence: snwu@mail.ncku.edu.tw; Tel.: +886-6-235-3535 (ext. 5334)
† The authors contributed equally to this work.

Abstract: QO-58 (5-(2,6-dichloro-5-fluoropyridin-3-yl)-3-phenyl-2-(trifluoromethyl)-1H-pyrazolol[1,5-a]pyrimidin-7-one) has been regarded to be an activator of K_V7 channels with analgesic properties. However, whether and how the presence of this compound can result in any modifications of other types of membrane ion channels in native cells are not thoroughly investigated. In this study, we investigated its perturbations on M-type K^+ current ($I_{K(M)}$), Ca^{2+}-activated K^+ current ($I_{K(Ca)}$), large-conductance Ca^{2+}-activated K^+ (BK_{Ca}) channels, and *erg*-mediated K^+ current ($I_{K(erg)}$) identified from pituitary tumor (GH_3) cells. Addition of QO-58 can increase the amplitude of $I_{K(M)}$ and $I_{K(Ca)}$ in a concentration-dependent fashion, with effective EC_{50} of 3.1 and 4.2 μM, respectively. This compound could shift the activation curve of $I_{K(M)}$ toward a leftward direction with being void of changes in the gating charge. The strength in voltage-dependent hysteresis (V_{hys}) of $I_{K(M)}$ evoked by upright triangular ramp pulse (V_{ramp}) was enhanced by adding QO-58. The probabilities of M-type K^+ (K_M) channels that will be open increased upon the exposure to QO-58, although no modification in single-channel conductance was seen. Furthermore, GH_3-cell exposure to QO-58 effectively increased the amplitude of $I_{K(Ca)}$ as well as enhanced the activity of BK_{Ca} channels. Under inside-out configuration, QO-58, applied at the cytosolic leaflet of the channel, activated BK_{Ca}-channel activity, and its increase could be attenuated by further addition of verruculogen, but not by linopirdine (10 μM). The application of QO-58 could lead to a leftward shift in the activation curve of BK_{Ca} channels with neither change in the gating charge nor in single-channel conductance. Moreover, cell exposure of QO-58 (10 μM) resulted in a minor suppression of $I_{K(erg)}$ amplitude in response to membrane hyperpolarization. The docking results also revealed that there are possible interactions of the QO-58 molecule with the KCNQ or $K_{Ca}1.1$ channel. Overall, dual activation of $I_{K(M)}$ and $I_{K(Ca)}$ caused by the presence of QO-58 eventually may have high impacts on the functional activity (e.g., anti-nociceptive effect) residing in electrically excitable cells. Care must be exercised when interpreting data generated with QO-58 as it is not entirely KCNQ/K_V7 selective.

Keywords: QO-58 (5-(2,6-dichloro-5-fluoropyridin-3-yl)-3-phenyl-2-(trifluoromethyl)-1H-pyrazolol[1,5-a]pyrimidin-7-one; 5-(2,6-dichloro-5-fluoro-3-pyridinyl)-3-phenyl-2-(trifluoromethyl)-pyrazolo[1,5-a]pyrimidin-7(4*H*)-one); M-type K^+ current; voltage-dependent hysteresis; M-type K^+ channel; Ca^{2+}-activated K^+ current; large-conductance Ca^{2+}-activated K^+ channel

Citation: Wu, C.-L.; Fu, P.; Cho, H.-Y.; Chuang, T.-H.; Wu, S.-N. Evidence for Dual Activation of $I_{K(M)}$ and $I_{K(Ca)}$ Caused by QO-58 (5-(2,6-Dichloro-5-fluoropyridin-3-yl)-3-phenyl-2-(trifluoromethyl)-1H-pyrazolol[1,5-a]pyrimidin-7-one). *Int. J. Mol. Sci.* **2022**, *23*, 7042. https://doi.org/10.3390/ijms23137042

Academic Editor: Michael Fromm

Received: 2 May 2022
Accepted: 22 June 2022
Published: 24 June 2022

1. Introduction

QO-58 (5-(2,6-dichloro-5-fluoropyridin-3-yl)-3-phenyl-2-(trifluoromethyl)-1*H*-pyrazolol[1,5-a]pyrimidin-7-one) has been demonstrated previously to be an opener of KCNQx

(K_V7x) channel [1–4]. It has been reported that this compound could increase the pain threshold of neuropathic pain in a rat model (i.e., chronic constriction injury of the sciatic nerve) [2]. It could also exercise anti-nociceptive action on inflammatory pain in rodents [5,6]. The ameliorating effects of this compound have been viewed to be closely linked to its activation of KCNQ (K_V7) channels [4,7,8]. However, QO-40 (5-(chloromethyl)-3-(nathphalen-1-yl)-2-(trifluoromethyl)pyrazolo[1,5-a]pyrimidin-7(4*H*)-one), a compound structurally similar to QO-58, has been noticeably reported to stimulate the activity of large-conductance Ca^{2+}-activated K^+ (BK_{Ca}) channels [9]. Therefore, whether and to what extent QO-58 is able to modify the amplitude or gating kinetics on different types of membrane ion currents remain to be not thoroughly explored.

It has been demonstrated that the KCNQ2, KCNQ3, or KCNQ5 encodes the core subunit of $K_V7.2$, $K_V7.3$, or $K_V7.5$ channel. The enhanced activity of this family of voltage-gated K^+ channels (KCNQx, K_V7x, or K_M [M-type K^+] channels) can generate macroscopic M-type K^+ current ($I_{K(M)}$), which is biophysically characterized by current activation upon low-threshold voltage [10,11]. Once being evoked during membrane depolarization, this type of K^+ currents, which is susceptible to block by linopirdine, has been disclosed to exhibit a slowly activating and deactivating property as well to affect the bursting patterns in different types of neurons, and endocrine or neuroendocrine cells [12–20]. Moreover, targeting $I_{K(M)}$ has been growingly thought to be an adjunctive regimen for the management of varying neurological, smooth muscle, or endocrine disorders which are closely linked to membrane hyperexcitability. These disorders include neuropathic pain and epilepsy [4,11,19,21–34]. A series of pyrazolopyrimidines or several botanical folk medicines have been also recently demonstrated to be KCNQ channel modulators [35,36]. KCNQ2/3 has been previously shown to be functionally active in different types of pituitary cells [15,29,37–39]. As such, whether and how the QO-58 can modulate the magnitude, gating, and voltage-dependent hysteresis (V_{hys}) of $I_{K(M)}$ residing in different types of electrically excitable cells are worthy of being further investigated.

The big-, high-, or large-conductance Ca^{2+}-activated K^+ (BK_{Ca} or BK) channels ($K_{Ca}1.1$, KCNMA1, *Slo1*) belong to a family of voltage-activated K^+ channels, and their activity can be increased by the elevation of intracellular Ca^{2+}, membrane depolarization, or both. Due to its high conductance, the BK_{Ca} channel is hence regarded as a maxi- or large-K^+ channel. The activity of these channels is abundantly and functionally distributed in an array of excitable and non-excitable cells. The regulation of such activity can play essential roles in various physiological or pathophysiological events, such as membrane excitability, neurotransmitter release, stimulus-secretion coupling, muscle relaxation, and pain sensation [40–46]. Moreover, some small molecules, such as BMS-204352, naringenin and QO-40, have been reported to activate $I_{K(M)}$ as well as to enhance the activity of BK_{Ca} channels in excitable cells [9,47,48].

The *erg* (*ether-à-go-go* related gene)-mediated K^+ current ($I_{K(erg)}$), the components for which are encoded by three different subfamilies of the KCNH gene, is able to generate the pore-forming α-subunit of *erg*-mediated K^+ (i.e., K_{erg} or K_V11) channels [49]. The $I_{K(erg)}$ is intrinsically present in different types of excitable cells. It can be engaged in the maintenance of resting potential and in modifications of the subthreshold excitability [50,51]. Whether the presence of QO-58 changes the magnitude of this type of K^+ current is largely unknown.

Therefore, the overall objective of this study was to explore possible underlying mechanism of QO-58 actions on different ionic currents (e.g., $I_{K(M)}$, $I_{K(Ca)}$, and $I_{K(erg)}$) present in excitable cells (e.g., pituitary GH_3 somatolactotrophs). The investigations obtained in this study showcase the evidence demonstrating that QO-58 is capable of interacting with K_M or BK_{Ca} channels to stimulate the amplitude of $I_{K(M)}$ or $I_{K(Ca)}$, respectively, in a concentration-dependent manner in these cells. In addition to the activation of M-type K^+ (K_M, KCNQ or K_V7) channels, QO-58-mediated activation of BK_{Ca}-channel activity is likely to converge to act on the functional activities of different types of excitable cells.

2. Results

2.1. Stimulatory Effect of QO-58 on M-Type K⁺ Current ($I_{K(M)}$) Recorded from Pituitary GH_3 Cells

In an initial stage of experiments, we wanted to test if the exposure to QO-58 produced any adjustments on the magnitude of $I_{K(M)}$ identified in these cells. To amplify $I_{K(M)}$ amplitude [31,52], we used high-K^+ (145 mM), Ca^{2+}-free solution as a bathing medium, and the recording pipette was filled up with a K^+-containing solution. As illustrated in Figure 1, one minute after addition of QO-58 (1 or 3 μM), the $I_{K(M)}$ magnitude evoked in response to 1-s depolarizing step from −50 to −10 mV progressively increased. For example, under cell exposure to 3 μM QO-58, $I_{K(M)}$ amplitude was evidently increased, as demonstrated by a considerable raise in the amplitude to 201 ± 26 pA (n = 8, p < 0.05) from a control value of 118 ± 19 pA (n = 8). The QO-58-mediated increase in $I_{K(M)}$ observed herein was also accompanied by the fastened activation time course of the current, as demonstrated by a shortening in the value of activation time constant (τ_{act}) from 68 ± 8 to 22 ± 4 ms (n = 8, p < 0.05) during exposure to 3 μM QO-58. After washout of QO-58, current amplitude returned to 122 ± 21 pA (n = 8, p < 0.05). Moreover, QO-58-mediated stimulation of $I_{K(M)}$ was attenuated by further addition of thyrotropin releasing hormone (TRH, 1 μM) or linopirdine (10 μM), but not by iberiotoxin (200 nM). The results were demonstrated by a decrease of current amplitude during further exposure to 1 μM TRH or 10 μM linopirdine to 125 ± 21 pA (n = 8, p < 0.05) or 127 ± 21 pA (n = 8, p < 0.05), respectively. TRH or linopirdine was reported to suppress $I_{K(M)}$ effectively in pituitary lactotrophs [18,31,49], while iberiotoxin is known to block large-conductance Ca^{2+}-activated K^+ (BK_{Ca}) channels.

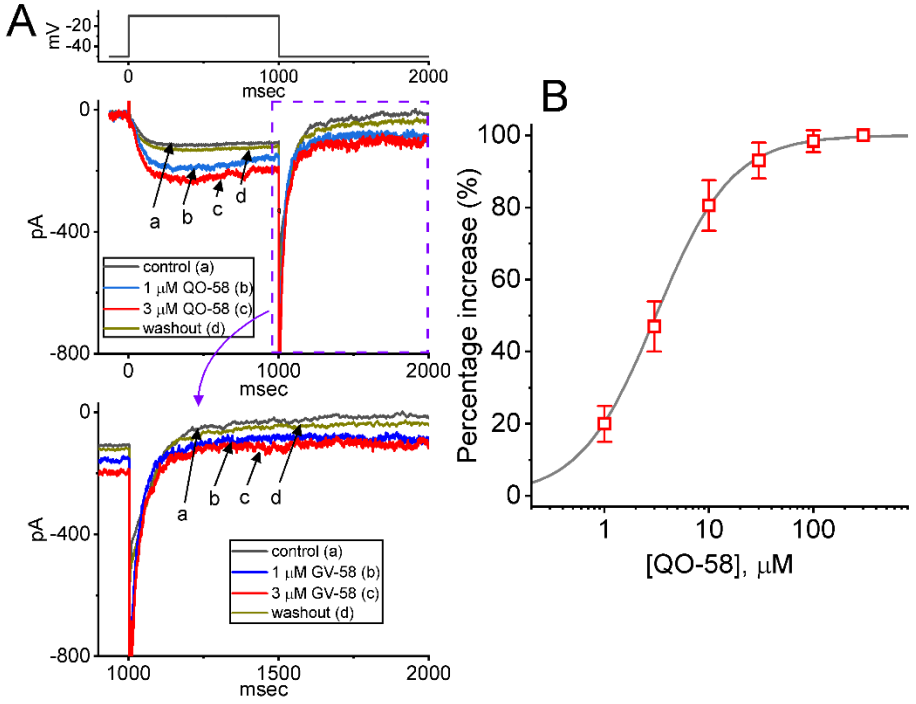

Figure 1. QO-58-induced stimulation of M-type K^+ current ($I_{K(M)}$) recorded from pituitary GH_3 cells. In these experiments, we placed cells in high-K^+ (145 mM), Ca^{2+}-free solution that contained 1 μM tetrodotoxin (TTX) and 0.5 mM $CdCl_2$ and the electrodes that we used were filled up with a K^+-containing solution. (**A**) Superimposed current traces obtained in the control period (a), during cell exposure of 1 μM QO-58 (b) or 3 μM QO-58 (c), and washout of QO-58 (d). The top part indicates the voltage-clamp protocol applied, while the lower part is an expanded record from purple dash box in the upper part. (**B**) Concentration-dependent stimulation of QO-58 effect on the amplitude of $I_{K(M)}$ (mean ± SEM; n = 8 for each point). Current amplitudes during cell exposure to different QO-58 concentrations were measured at the end of depolarizing pulse from −50 to −10 mV with a duration of 1 s. Sigmoid smooth curve indicates best fit to a modified Hill function described in Section 4.

The relationship between the QO-58 concentration and the percentage increase of $I_{K(M)}$ was ascertained and is hence illustrated in Figure 1B. To evoke $I_{K(M)}$ obtained in the control period (i.e., absence of QO-58) and during cell exposure to different concentrations (1–300 μM) of QO-58, each cell was depolarized from −50 to −10 mV with a duration of 1 s. Addition of QO-58 was noticed to increase the amplitude of $I_{K(M)}$ in a concentration-dependent fashion. As the data became least-squares fitted to a Hill function as stated in Section 4, the half-maximal concentration (i.e., EC_{50}) required for stimulatory effect of QO-58 on $I_{K(M)}$ was calculated to be 3.1 μM. The data from this set of experiments reflect that QO-58 has a stimulatory effect on $I_{K(M)}$ in GH_3 cells in a concentration-dependent manner.

2.2. Effect of QO-58 on Average Current Versus Voltage (I-V) Relationship and Steady-State Activation Curve of $I_{K(M)}$

We next continued to study if the presence of QO-58 can modify the $I_{K(M)}$ amplitude measured at different levels of membrane potentials. The average *I-V* relationship of $I_{K(M)}$ with or without the QO-58 application is illustrated in Figure 2A. The current amplitude noticeably arose as the membrane potential became depolarized to −30 mV, and the magnitude of QO-58-stimulated $I_{K(M)}$ at the level of −10 mV was higher than that at −20 or −30 mV. The relationship of relative $I_{K(M)}$ conductance versus membrane potential acquired in the control period (i.e., QO-58 was not present) and during cell exposure to 3 μM QO-58 was constructed (Figure 2B). The continuous sigmoidal curve derived from experimental data sets was optimally fitted with a modified Boltzmann function (described in Section 4). In control, $V_{1/2}$ = −18.3 ± 0.7 mV (n = 8), q = 6.2 ± 0.2 e (n = 8), and in the presence of 3 μM QO-58, $V_{1/2}$ = −28.5 ± 0.8 mV (n = 8), q = 6.1 ± 0.2 e (n = 8). The results enabled us to reflect that in addition to increasing $I_{K(M)}$ conductance, the presence of QO-58 could exert a leftward shift (approximately 10 mV) along the voltage axis in the activation curve of the current, albeit with no change in the gating charge of the activation curve.

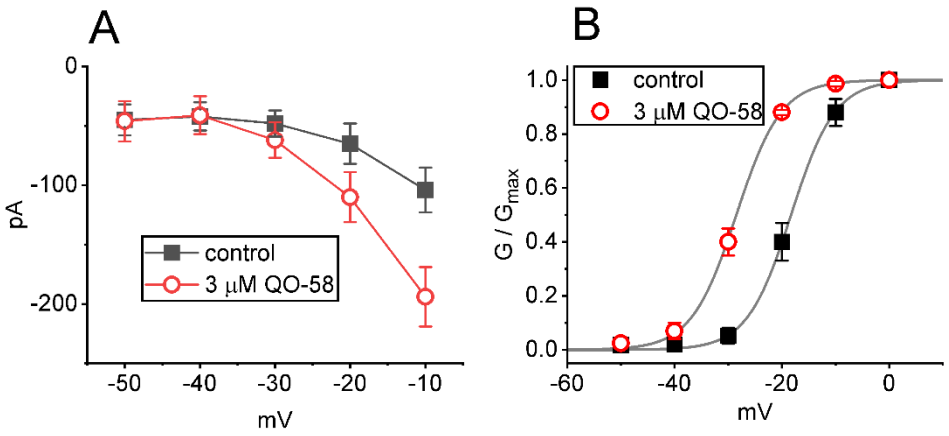

Figure 2. Effect of QO-58 on the current versus voltage (*I-V*) relationship (**A**) and the activation curve (**B**) of $I_{K(M)}$. The experimental protocol applied is the same as that used in Figure 1. (**A**) Average *I-V* relationship of $I_{K(M)}$ amplitude acquired in the control period (i.e., absence of QO-58, solid black squares) and during cell exposure to 3 μM QO-58 (open red circles). (**B**) Steady-state activation curve of $I_{K(M)}$ in the absence (solid black squares) and presence (open red circles) of 3 μM QO-58 (mean ± SEM; n = 8). Smooth curves drawn were optimally fitted to a modified Boltzmann function as elaborated in Section 4. Of note, there is a leftward shift along the voltage axis in the quasi-steady-state activation curve of $I_{K(M)}$ in QO-58 presence, despite being void of changes in the gating charge of the curve.

2.3. Effect of QO-58 on $I_{K(M)}$ Triggered by Triangular Ramp Pulse (V_{ramp}) with Varying Durations

Earlier reports have shown the capability of $I_{K(M)}$ strength to modulate the patterns of bursting firing in central neurons [13,15–17,20]. Therefore, we continued to evaluate how the presence of QO-58 could have any perturbations on $I_{K(M)}$ responding to upright

triangular V_{ramp} with varying durations. These V_{ramp} waveforms were specifically designed and, during the measurements, thereafter, delivered to the tested cell through digital-to-analog conversion. In the current experimental scenario, we voltage-clamped the cell at −50 mV, and the upsloping (forward) limb from −50 to 0 mV followed by the downsloping (reverse) limb back to −50 mV with varying duration (0.4–3.2 s) was imposed over it. As demonstrated in Figure 3, the peak amplitude of $I_{K(M)}$ became progressively declined with increasing the V_{ramp}'s duration (or decreasing the V_{ramp}'s speed); however, as the V_{ramp}'s slope decreased, the maximal strength of $I_{K(M)}$ triggered by the upsloping limb of triangular V_{ramp} progressively increased. Moreover, it can be seen that under cell exposure to 3 μM QO-58, the current magnitude responding to both rising and falling V_{ramp} was increased (Figure 3A,B). For example, as the during of triangular V_{ramp} was set at 3.2 s (i.e., slope = 31.25 mV/s), the application of 3 μM QO-58 increased the current amplitude measured from the upsloping or downsloping limb at the level of −10 mV from 63 ± 4 to 81 ± 5 pA (n = 8, $p < 0.05$) or from 91 ± 6 to 148 ± 11 pA (n = 8, $p < 0.05$), respectively. The experimental observations project that the strength of $I_{K(M)}$ in the upsloping limb was obviously increased as the duration of triangular V_{ramp} increased, while that in the downsloping end progressively decreased, and that the presence of QO-58 contributed to an increase in $I_{K(M)}$ in a time- and state-dependent manner in GH_3 cells.

The voltage-dependent hysteresis (V_{hys}) of ionic currents have been growingly noticed to exert important impacts on electrical behaviors of action potential firing [29,31,53,54]. As illustrated in Figure 3A,B, the $I_{K(M)}$ amplitude triggered by the upsloping limb of upright triangular V_{ramp} was evidently lower than that by the downsloping end, strongly reflecting that a V_{ramp}-induced V_{hys} behavior resides in $I_{K(M)}$ observed in GH_3 cells. As the duration of triangular V_{ramp} increased from 0.4 to 3.2 s (i.e., the V_{ramp}'s slope became decreased), the V_{hys} degree was reduced. Of notice, by adding QO-58 (3 μM), $I_{K(M)}$ evoked during the upsloping limb of triangular V_{ramp} arose to a less extent than that measured at the downsloping ramp. For example, in control period (i.e., absence of QO-58), $I_{K(M)}$ at the level of −15 mV during the upsloping and downsloping ends of triangular V_{ramp} were 53 ± 6 pA (n = 8) and 91 ± 8 pA (n = 8), respectively, the values between which were noticed to differ significantly ($p < 0.05$). Moreover, by adding QO-58 (3 μM), the amplitudes of forward and backward $I_{K(M)}$ at the same level of voltage noticeably increased to 69 ± 7 pA (n = 8, $p < 0.05$) and 138 ± 11 pA (n = 8, $p < 0.05$), respectively. Therefore, the magnitude of QO-58-mediated current stimulation at the upsloping (forward) and downsloping (backward) limbs of triangular V_{ramp} differ significantly. The presence of 3 μM QO-58 increased $I_{K(M)}$ amplitude at −15 mV during the upsloping or downsloping limb of triangular V_{ramp} by about 16% or 52%, respectively.

We further quantified the degree (i.e., V_{hys}'s Δarea) of V_{ramp}-induced V_{hys} of $I_{K(M)}$. The results demonstrated that the amount of V_{hys} responding to 3.2 s triangular V_{ramp} was considerably increased in the presence of QO-58. Figure 3C summarizes the data demonstrating the effects of QO-58 (1 or 3 μM) on the area encircling the forward and backward current trajectory of V_{ramp}-evoked $I_{K(M)}$. For example, in addition to its stimulation of $I_{K(M)}$ amplitude, cell exposure of 3 μM QO-58 resulted in an increase in the V_{hys} strength responding to long-lasting triangular V_{ramp}, as illustrated by a considerable increase in V_{hys}'s Δarea arising from 508 ± 26 to 939 ± 41 mV·pA (n = 8, $p < 0.05$). Moreover, during the continued exposure to 3 μM QO-58, subsequent exposure to 10 μM linopirdine appreciably attenuated the Δarea to 612 ± 33 mV·pA (n = 8, $p < 0.05$). Linopirdine was reported to be a blocker of K_M channels [18]. It is plausible to assume, therefore, that QO-58 is effective in stimulating $I_{K(M)}$ residing in GH_3 cells in a V_{hys}-dependent manner.

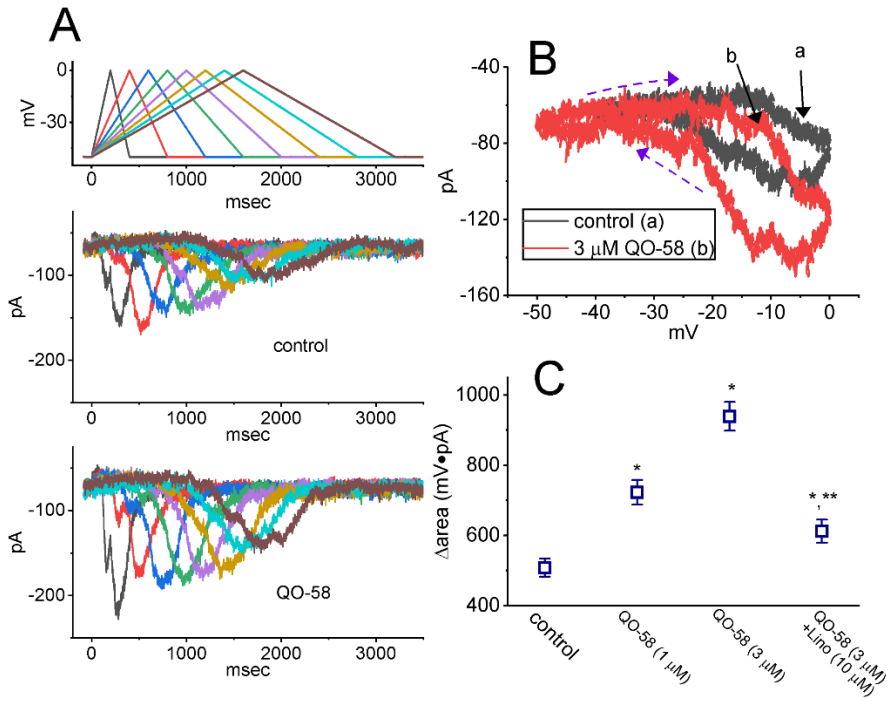

Figure 3. Effect of QO-58 on $I_{K(M)}$ in response to an upright isosceles-triangular ramp pulse (V_{ramp}) observed in GH_3 cells. The V_{ramp} with different durations (0.4–3.2 s) (or with ramp speed between ±31.25 and ±250 mV/s) was designed to mimic different depolarizing and repolarizing slopes in bursting patterns of neuronal firing. (**A**) Representative $I_{K(M)}$ traces in response to the double-pulse V_{ramp} in the absence (upper) and presence (lower) of 3 μM QO-58. The voltage protocol used is indicated in the uppermost part, and voltage waveforms appearing in different colors are indicated to correspond with current traces evoked by the waveforms. (**B**) Effect of QO-58 (3 μM) on voltage-dependent hysteresis (V_{hys}) (i.e., the relationship of forward and backward current versus membrane voltage) of $I_{K(M)}$ evoked by triangular V_{ramp} with a duration of 3.2 s. Black or red current trajectory indicates the absence or presence of 3 μM QO-58, respectively. The direction of $I_{K(M)}$ in which time passes during the elicitation by 3.2 s triangular V_{ramp} is indicated by dashed arrows. (**C**) Summary scatter graph showing the effect of QO-58 on the V_{hys}'s Δarea (mean ± SEM; n = 8 for each point). Δarea means the area encircling the forward (upsloping) and backward (downsloping) limbs of current trajectory evoked by V_{ramp}. * Significantly different from control ($p < 0.05$), and ** significantly different from 3 μM QO-58 alone group ($p < 0.05$).

2.4. Effect of QO-58 on M-Type K^+ Channel (K_M) Channels Measured from GH_3 Cells

The QO-58-stimulated whole-cell $I_{K(M)}$ detected above in these cells could arise from changes occurring in either channel open probability, single-channel amplitude, gating kinetics, or the number of K_M channel. The reasons therefore enabled us to investigate the single-channel recordings of the channel with or without the presence of QO-58. In this set of cell-attached current recordings, we placed cells in high-K^+, Ca^{2+}-free solution, and the recording pipette was filled with low-K^+ (5.4 mM) solution. As demonstrated in Figure 4A, when the examined cell was maintained at +20 mV relative to the bath, the activity of single K_M channel was robustly observed [31,55]. Of particular interest, as QO-58 was applied to the bath, the probabilities of K_M-channel openings progressively increased. For example, the presence of 3 μM QO-58 significantly increased the channel open probability from 0.087 ± 0.021 to 0.238 ± 0.041 (n = 8, $p < 0.05$); however, there was devoid of changes in single-channel amplitude (Figure 4B). Moreover, in continued presence of 3 μM QO-58, linopirdine (10 μM) resulted in an attenuation of QO-58-stimulated channel activity, as demonstrated in a significant reduction in channel activity to 0.164 ± 0.025 (n = 8, $p < 0.05$).

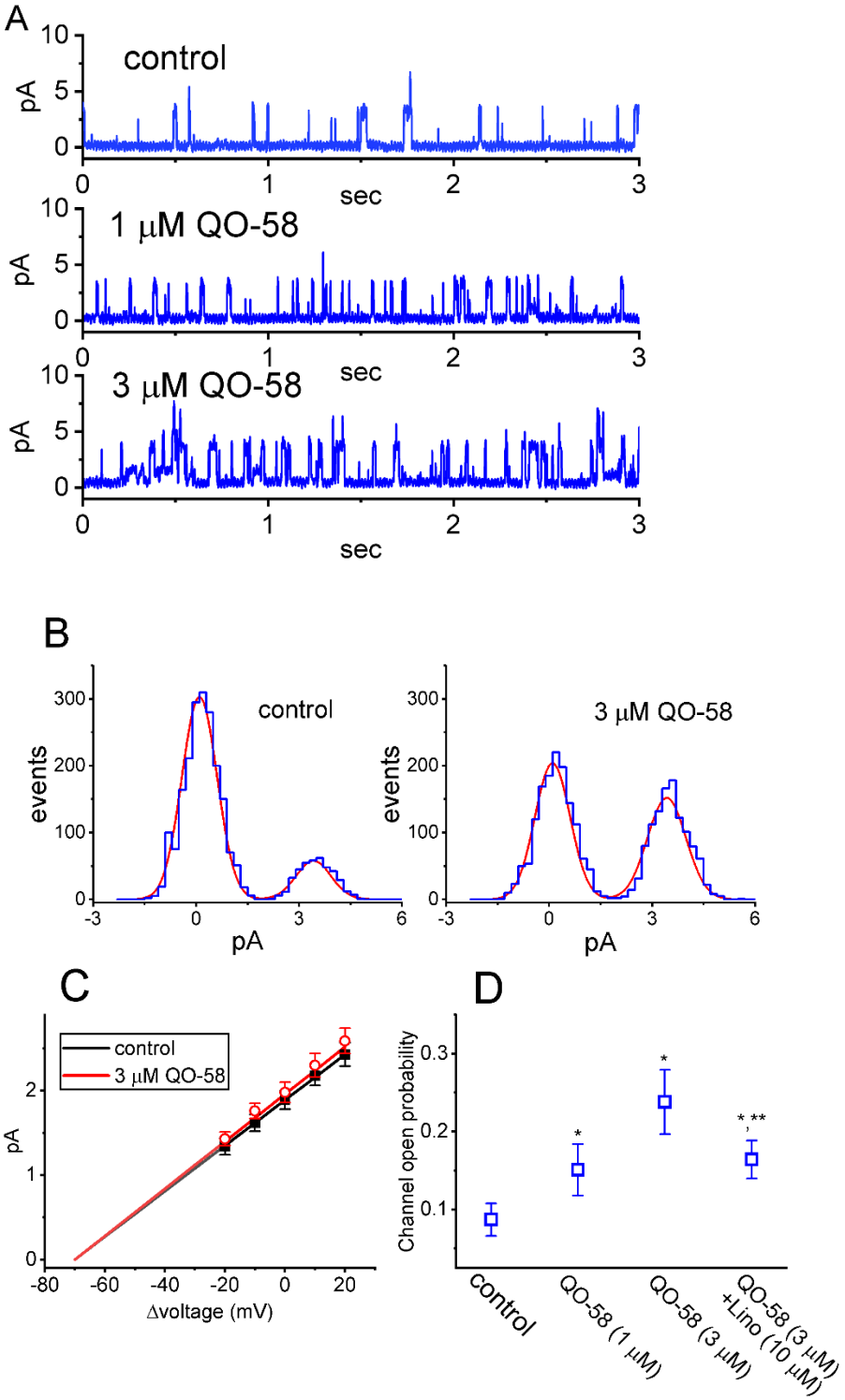

Figure 4. Stimulatory effect of QO-58 on the activity of M-type K^+ (K_M) channels recorded from GH_3 cells. In this series of cell-attached current recordings, cells were bathed in high-K^+, Ca^{2+}-free solution, and we filled up the recording pipette with low-K^+ (5.4 mM) solution. (**A**) Representative single K_M channels in the control period (upper) and during cell exposure to 1 μM QO-58 (middle) or 3 μM QO-58 (lower). The channel activity in the absence or presence of QO-58 was taken at the level of +20 mV relative to the bath. The upward deflection indicates the opening event of the channel. (**B**) Amplitude histogram taken in the absence (left) and presence (right) of 3 mM QO-58. (**C**) Average *I-V* relationship of single K_M channels in the absence (solid black squares) and presence (open red circles) of 3 μM QO-58 (mean ± SEM; n = 8 for each point). Of note, the linear relationship of K_M channels

versus Δvoltage was superimposable between the absence and presence of QO-58; hence, the single-channel conductance of the channel between the absence and presence of 3 μM QO-58 did not differ. (**D**) Summary scatter graph showing effect of QO-58 (1 and 3 μM) and QO-58 (3 μM) plus linopirdine (Lino, 10 μM) on the probability of K_M channels that would be open (mean ± SEM; $n = 8$ for each point). Channel activity was measured at +20 mV relative to the bath. * Significantly different from control ($p < 0.05$) and ** significantly different from QO-58 (3 μM) alone group ($p < 0.05$).

2.5. Effect of QO-58 on the Single-Channel Conductance and Activation Curve of K_M Channels

We further examined if K_M-channel activity measured at different levels of membrane potentials could be altered by the presence of QO-58. As demonstrated in Figure 4C, the single channel conductance of K_M channels achieved with or without application of QO-58 did not significantly differ (27 ± 3 pS [in control] versus 28 ± 3 pS [in the presence of 3 μM QO-58]; $n = 8$, $p > 0.05$), despite the increased probability of K_M-channel openings in its presence. A summary showing effects of QO-58 and QO-58 plus linopirdine on K_M-channel activity in GH_3 cells is also presented in Figure 4D. The results led us to reflect that as GH_3 cells were continually exposed to QO-58 (3 μM), the channel open probability was significantly attenuated by subsequent addition of linopirdine (10 μM).

2.6. QO-58-Mediated Stimulation of Ca^{2+}-Activated K^+ Currents ($I_{K(Ca)}$) by the Presence of QO-58

Several small molecules (e.g., BMS-204352, naringenin, and QO-40) that demonstrated to stimulate K_M-channel activity have been reportedly noted to regulate other types of K^+ currents (e.g., $I_{K(Ca)}$) [9,47,48]. For these reasons, we next explored if QO-58 is able to modify the amplitude of $I_{K(Ca)}$ residing in GH_3 cells. In these experiments we voltage-clamped the tested cell at a holding potential of 0 mV to prevent the interference by other type of ionic currents (i.e., voltage-gated Ca^{2+} currents) [56,57]. As demonstrated in Figure 5A, one minute after cell exposure to 3 μM QO-58, $I_{K(Ca)}$ amplitudes measured at different levels of membrane potentials increased. Average *I-V* relationships of $I_{K(Ca)}$ with or without the QO-58 (3 μM) presence are illustrated in Figure 5B. The concentration-dependent stimulation by QO-58 of macroscopic $I_{K(Ca)}$ amplitude was established and is hence depicted in Figure 5C. According to the Hill equation described in Section 4, the EC_{50} value required for QO-58-stimulated effect on $I_{K(Ca)}$ was calculated to be 4.2 μM.

2.7. Stimulatory Effect of QO-58 on the Activity of Large-Conductance Ca^{2+}-Activated K^+ (BK_{Ca}) Channels Identified in GH_3 Cells

The QO-58-induced raise in whole-cell $I_{K(Ca)}$ described above could be mediated through either adjustment in channel open probability, single-channel amplitude, gating kinetics of the BK_{Ca} channels, or in any combinations. Therefore, these reasons urged us to assess the single-channel activities of the channels functionally active in GH_3 cells. In this set of inside-out current recordings, we bathed the tested cells in high-K^+ solution containing 0.1 μM Ca^{2+}, and the recording pipette was filled up with K^+-containing solution. As demonstrated in Figure 6A, as the excised patch was voltage-clamped at +60 mV, the activity of BK_{Ca} channels occurring in rapid and independent open-closed transitions was robustly detected. One minute after bath addition of QO-58, the channel opening probability was conceivably increased. For example, under inside-out configuration, QO-58 at a concentration of 1 or 3 μM applied to bath medium led to a respective increase in channel opening probability to 0.118 ± 0.005 ($n = 8$, $p < 0.05$) or 0.174 ± 0.006 ($n = 8$, $p < 0.05$) from a control value of 0.073 ± 0.004 ($n = 8$). However, single-channel amplitude of BK_{Ca} channel was not noticed to differ significantly between the absence and presence of 3 μM QO-58 (12.8 ± 2 pA [in control] versus 12.9 ± 2 pA [in the presence of 3 μM QO-58]; $n = 8$, $p > 0.05$). Under the exposure to 3 μM QO-58, the slow component of mean closed time of the channel became considerably shortened to 19 ± 3 ms ($n = 8$, $p < 0.05$) from a control value of 32 ± 5 ms ($n = 8$). Of additional notice, as the excised patch was continually exposed to 3 μM QO-58, subsequent addition of verruculogen (1 μM) considerably decreased

channel open probability to 0.074 ± 0.004 (n = 8, $p < 0.05$), although further application of linopirdine (10 μM) produced minimal effect on it (0.174 ± 0.006 [in the presence of 3 μM QO-58 alone] versus 0.173 ± 0.006 [in presence of QO-58 plus linopirdine]; n = 8, $p > 0.05$) (Figure 6B). Verruculogen is a tremorgenic mycotoxin known to effectively suppress the activity of BK_{Ca} channels [58,59]. Therefore, the experimental results strongly indicate that QO-58-activated channel activity is mainly through its activation of BK_{Ca} channels, rather than that of K_M channels. They also enable us to project that the activation is attributed primarily to the shortening of mean closed time of the channel, despite no change in single-channel amplitude in the presence of QO-58.

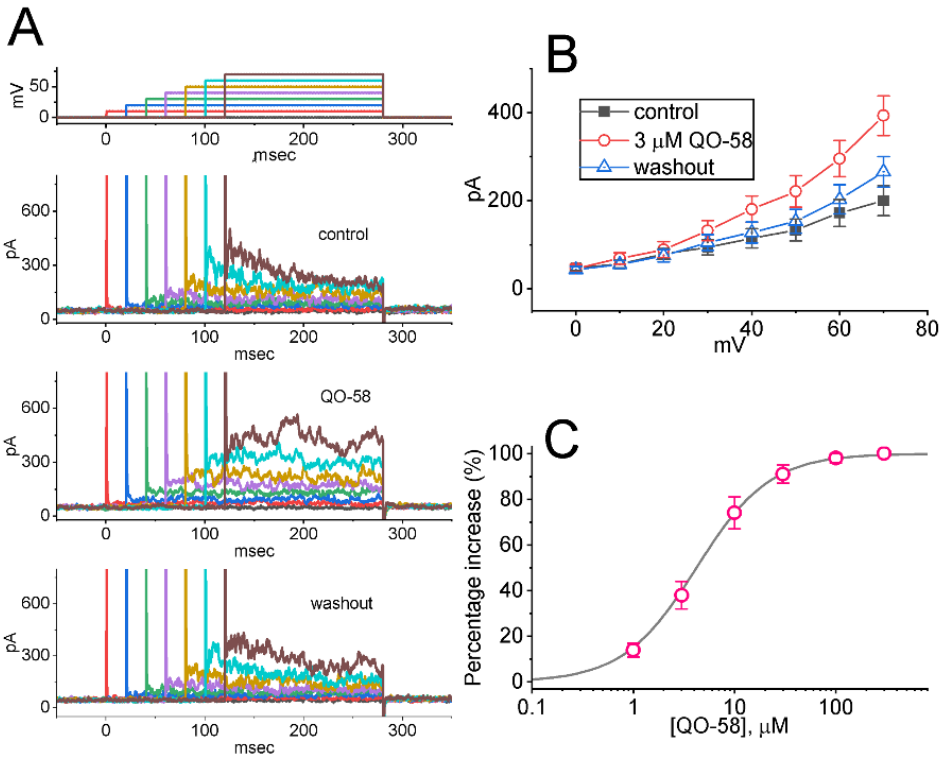

Figure 5. Stimulatory effect of QO-58 on the amplitude of whole-cell (i.e., macroscopic) Ca^{2+}-activated K^+ current ($I_{K(Ca)}$) measured from GH_3 cells. In this series of voltage-clamp current recordings on these cells, we used normal Tyrode's solution containing 1.8 mM $CaCl_2$ as a bathing medium, and the recording pipette used was backfilled with K^+-enriched solution. As whole-cell configuration was established, we evoked $I_{K(Ca)}$ from a holding potential of 0 mV to test potentials in the range of 0 and +70 mV (10-mV in increments) at a rate of 0.1 Hz. (**A**) Superimposed current traces activated in response to a series of voltage steps (indicated in the uppermost part). Current traces in the upper part are controls (i.e., absence of QO-58), those in the middle part were recorded during cell exposure to 3 μM QO-58, while those in lower part were taken after washout of the QO-58. The duration of rectangular voltage commands applied was set in the range of 280 and 160 ms (20-ms decrements), indicating a progressive increase with membrane depolarization (i.e., an outwardly-rectifying property). (**B**) Average *I-V* relationship of $I_{K(Ca)}$ obtained in the control period, during the exposure to 3 μM QO-58, and after washout of QO-58. Current amplitude was measured at the end of each depolarizing pulse. Each point represents the mean ± SEM (n = 8). (**C**) Concentration-response relationship for QO-58-induced stimulation of $I_{K(Ca)}$ (mean ± SEM; n = 8 for each point). The gray continuous line drawn is reliably fitted to the Hill equation. The values for EC_{50} or n_H were yielded to be 4.2 μM or 1.2, respectively.

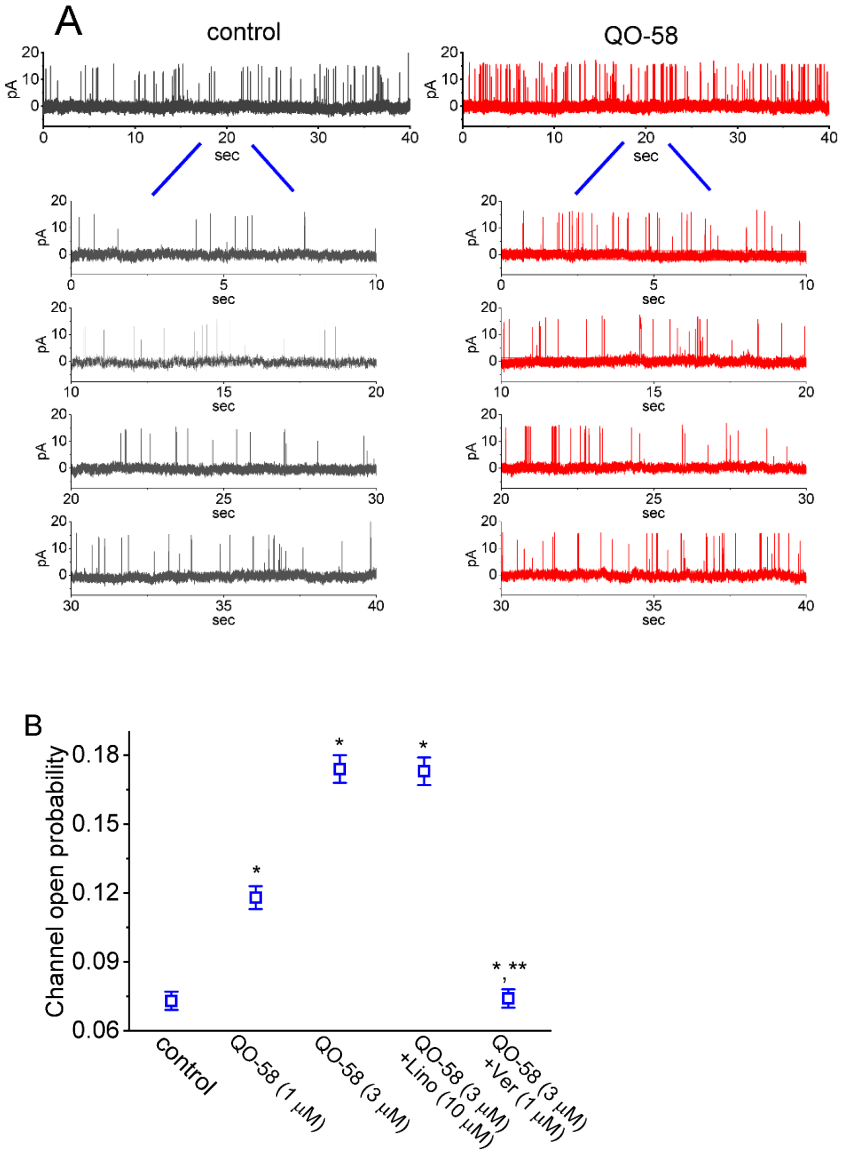

Figure 6. Stimulatory effect of QO-58 on the activity of BK_{Ca} channels recorded from GH_3 cells. We conducted these inside-out current recordings in cells which were bathed in high-K^+ solution containing 0.1 μM Ca^{2+}, and the recording pipette was then filled up with K^+-containing solution. (**A**) Original BK_{Ca}-channel currents obtained in the control period (left, black color) and after bath application of 3 μM QO-58 (right, red color). The detached patch was voltage-clamped at +60 mV. The lower part indicates the expanded records from the uppermost part. The opening event of the channel is indicated by the upward deflection. (**B**) Summary scatter graph showing effect of QO-58, QO-58 plus linopirdine (Lino), or QO-58 plus verruculogen (Ver) (mean ± SEM; $n = 8$ for each point). Under inside-out configuration, the channel open probability was measured at the level of +60 mV. * Significantly different from control ($p < 0.05$) and ** significantly different from QO-58 (3 μM) alone group ($p < 0.05$).

We further explored how the presence of QO-58 alters BK_{Ca}-channel activity at different levels of membrane potentials. As demonstrated in Figure 7A, the linear relationship of single-channel amplitude versus membrane potential (i.e., single-channel conductance) was collated under inside-out configuration. As the excised patch was exposed to 3 μM QO-58, the value of single-channel conductance obtained between the absence and presence of QO-58 did not differ significantly (213 ± 8 pS [in control] versus 215 ± 9 pS [in the presence of QO-58]; $n = 8$, $p > 0.05$). Additionally, the steady-state activation curve of BK_{Ca} channels with or with the QO-58 application is illustrated in Figure 7B. As the smooth lines drawn

by fitting the data to the Boltzmann equation stated in Section 4, the results demonstrated that during the exposure to QO-58, there was a leftward shift (approximately 14 mV) along the voltage axis in the activation curve of the channel with no appreciable modifications in gating charge. For example, in control, $V_{1/2}$ = +66 ± 8 mV and q = 4.9 ± 0.2 e (n = 8), while in the presence of 3 µM QO-58, $V_{1/2}$ = +52 ± 7 mV and q = 4.8 ± 0.2 e (n = 8). These results indicated that although neither single-channel conductance nor gating charge of the channel was changed, the steady-state activation curve of BK_{Ca} channels measured under inside-out excised patch of GH_3 cells was shifted toward less depolarized potential, as the detached patch was exposed to QO-58.

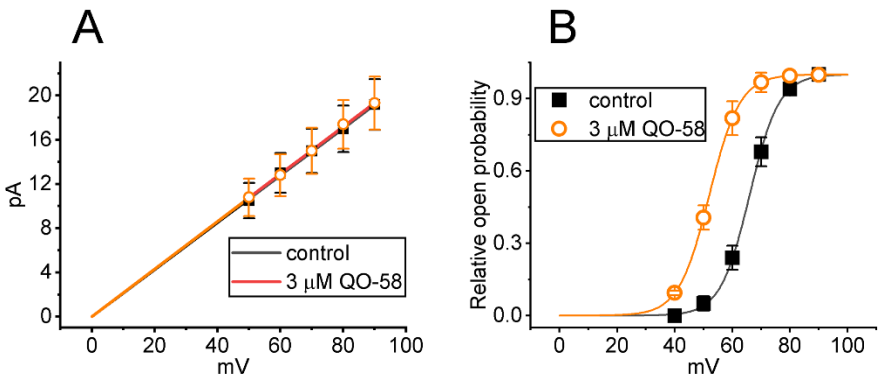

Figure 7. Effect of QO-58 on single-channel conductance (**A**) and activation curve (**B**) of BK_{Ca} channels in GH_3 cells. In this series of inside-out current recordings, we voltage-clamped the excised patched at different levels of membrane potentials, and the recording pipette was filled with K^+-enriched solution. (**A**) Average *I-V* relationship of single BK_{Ca}-channel currents (i.e., linear regression between membrane potential and mean single-channel amplitude) obtained in the absence (black filled squares) and presence (orange open circles) of 3 µM QO-58 (mean ± SEM; n = 8 for each point). Of note, the linear relationship of BK_{Ca} channels between the absence and presence of QO-58 is superimposed, and the value of reversal potential with or without the QO-58 addition was pointed toward zero mV. (**B**) Steady-state activation curve of BK_{Ca} channels obtained in the control period (black filled squares) and during exposure to 3 µM QO-58 (orange open circles) (mean ± SEM; n = 8 for each point). Sigmoid lines indicate the best fit to a Boltzmann function as stated in Section 4. Of note, there is a leftward shift of the activation curve of the channel, although neither single-channel conductance of the channel nor gating charge of the curve was altered by QO-58 presence.

2.8. Minor Inhibitory Effect of QO-58 on Erg-Mediated K^+ Current ($I_{K(erg)}$) Seen in GH_3 Cells

In another set of experiments, we attempted to explore if the presence of QO-58 could have any influence on another type of whole-cell K^+ current (i.e., $I_{K(erg)}$). The measurements were conducted in these cells bathed in high-K^+, Ca^{2+}-free solution containing 1 µM TTX and 0.5 mM $CdCl_2$, and the pipette that was used was filled up with K^+-enriched solution. The tested cell was voltage-clamped at −10 mV, and a series of command voltage steps ranging between −100 and 0 mV was thereafter delivered to evoke deactivating $I_{K(erg)}$ [12,37,52,60–63]. As illustrated in Figure 8, under cell exposure to 10 µM QO-58, average *I-V* relationship of $I_{K(erg)}$ became lessened in the voltages ranging between −100 and −50 mV. For example, at the level of −100 mV, the exposure to 10 µM QO-58 significantly reduced the peak amplitude of hyperpolarization-activated $I_{K(erg)}$ by 25 ± 2% from 1055 ± 139 to 791 ± 113 pA (n = 7, p < 0.05). After the compound's washout, current amplitude returned to 1012 ± 131 pA (n = 7, p < 0.05). Therefore, it is noticeable that unlike QO-58 effect on $I_{K(M)}$ or $I_{K(Ca)}$, $I_{K(erg)}$ functionally active in GH_3 cells is susceptible to minor inhibition by the QO-58 presence.

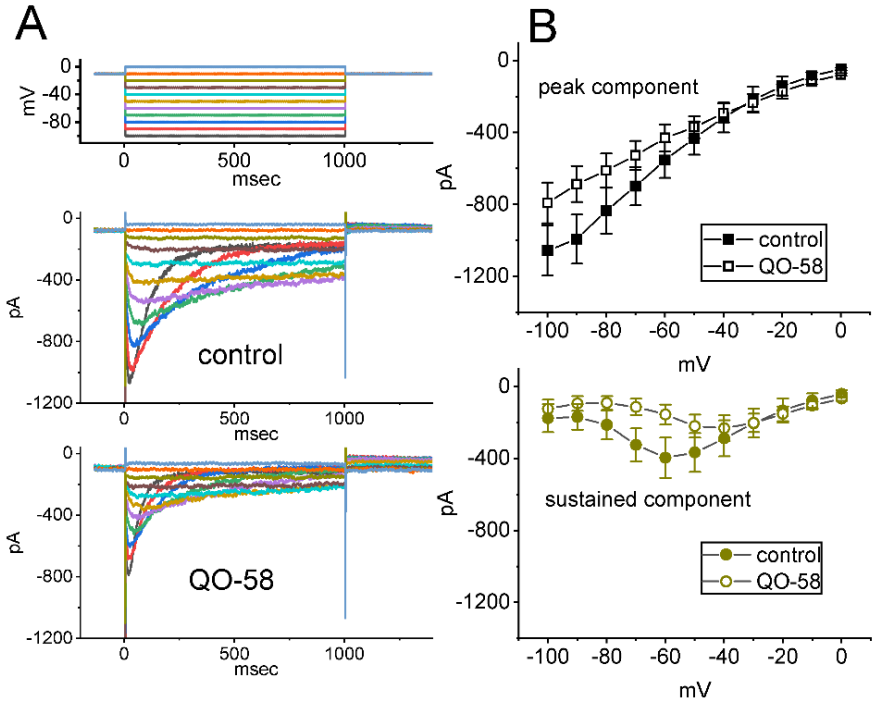

Figure 8. Minor inhibition of *erg*-mediated K^+ current ($I_{K(erg)}$) produced by the presence of QO-58 in GH_3 cells. In these experiments, we used high-K^+, Ca^{2+}-free solution as bathing medium and the recording pipette was filled up with K^+-containing (145 mM) solution. (**A**) Superimposed current traces obtained in the control period (upper) and during cell exposure to 10 μM QO-58 (lower). The top part indicates the voltage-clamp protocol imposed. (**B**) Average *I-V* relationship of peak (black squares, upper) or sustained (brown circles, lower) component of $I_{K(erg)}$ obtained in the absence (filled symbols) and presence (open symbols) of 10 μM QO-58 (mean ± SEM; $n = 7$ for each point). Peak or sustained $I_{K(erg)}$ obtained with or without the QO-58 addition was measured at the start or end-point of each hyperpolarizing step with a duration of 1 s. Of note, the presence of 10 μM QO-58 slightly inhibited $I_{K(erg)}$ in these cells.

2.9. Docking Results on Interaction between K_{Ca}1.1 Channel and QO-58 or between KCNQ2 and QO-58

In a final set of studies, we investigated how the protein of K_{Ca}1.1 (or α-subunit of BK_{Ca} channel) or KCNQ2 could be docked with QO-58 by exploiting PyRx software. The predicted binding sites of the QO-58 molecule were demonstrated in Figure 9. Of notice, with being docked to K_{Ca}1.1 with a binding energy of −7.1 kcal/mol, QO-58 can form hydrogen bond with residue Thr 277, while it is able to have hydrophobic contact with residue Thr 277, Val 302, Phe 305, Ala 306, Ala 309, and Gly 310. Alternatively, as being docked to KCNQ2 with a binding energy of −6.9 kcal/mol, QO-58 can form hydrophobic contact with residue Ile 381, Ser 382, Pro 383, Asn 384, Leu 385, and Leu 387. Of notice, these results thus prompted us to reflect that KCNQ2 and BK_{Ca} channels are likely to share unique motifs or recognition sequences with which QO-58 or other structurally similar compounds can interact, and that QO-58 can bind to the cytoplasmic residues of KCNQ2 or K_{Ca}1.1 channel, which are adjacent to transmembrane segment of the channel. Therefore, care needs to be mentioned in attributing the actions of QO-58 or other structurally similar compounds exclusively to the stimulation of KCNQx- (K_V7-) channel activity as reported previously [4,8,18].

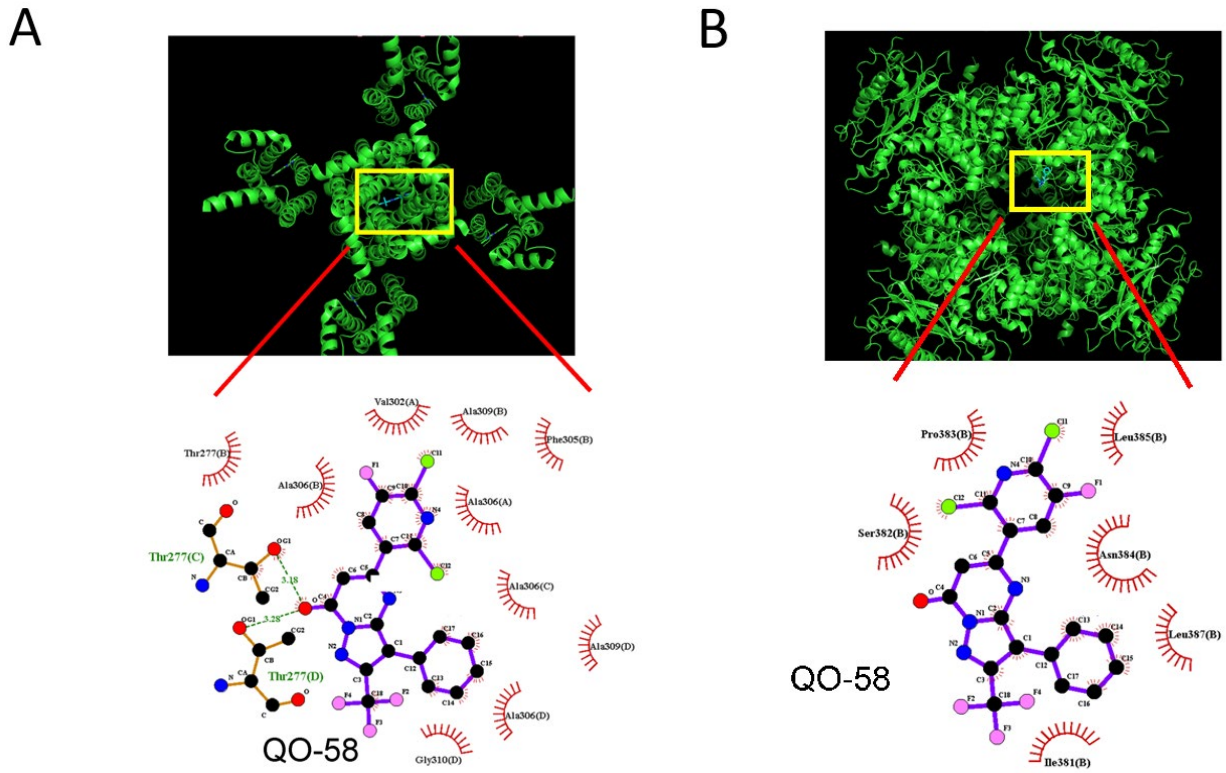

Figure 9. Docking results of $K_{Ca}1.1$ channel and QO-58 (**A**) or KCNQ2 and QO-58 (**B**). Protein structure of $K_{Ca}1.1$ or KCNQ2 channel was acquired from PDB (PDB ID: 6V3G or 7CR1), respectively, while chemical structure of QO-58 was from PubChem (Compound CID: 51351551). The structure of $K_{Ca}1.1$ or KCNQ2 channel was docked by the QO-58 molecule through PyRx (https://pyrx.sourceforge.io/, accessed on 23 June 2022). The diagram of interactions between $K_{Ca}1.1$ or KCNQ2 channel and the QO-58 molecule was generated by LigPlot$^+$ (https://www.ebi.ac.uk/thornton-srv/software/LIGPLOT/, accessed on 23 June 2022). Of note, the red arcs with spokes radiating toward the ligand (i.e., QO-58) in the lower part of each panel denote the hydrophobic contact, while green dot line indicates the hydrogen bond.

3. Discussion

The noticeable conclusions are drawn from this study as follows. First, the presence of QO-58 concentration-dependently increased the amplitude of $I_{K(M)}$ and $I_{K(Ca)}$ with EC_{50} value of 3.1 and 4.2 μM, respectively. Second, under cell exposure to QO-58, the steady-state activation curve of $I_{K(M)}$ was shifted along voltage axis to a hyperpolarized potential with no change in the gating charge. Third, the V_{hys} strength of $I_{K(M)}$ activated by triangular V_{ramp} measurably increased by the QO-58 presence. Fourth, cell exposure to QO-58 enhanced the probability of BK_{Ca}-channel openings as well as shifted the activation curve of the channel at steady state toward the less depolarized potential; however, neither the gating charge nor single-channel conductance of the channel was affected during its exposure. Fifth, the deactivating $I_{K(erg)}$ activated by membrane hyperpolarization was slightly suppressed by adding QO-58. Taken together, the interaction of QO-58 with K_M or BK_{Ca} channels to stimulate $I_{K(M)}$ or $I_{K(Ca)}$ in excitable cells is expected to occur in a concentration- and voltage-dependent manner, assuming that similar in vivo findings occur.

In agreement with previous studies [2], the current observations demonstrated that with optimum EC_{50} of 3.1 μM, QO-58 was capable of enhancing the magnitude of $I_{K(M)}$ seen in GH_3 cells. Furthermore, the V_{hys} changes have been regarded to play an essential characteristic in electrical behaviors of different excitable cells. In the current study, in accordance with earlier studies [29,31,53,54], the $I_{K(M)}$ intrinsically residing in GH_3 cells was robustly observed to undergo V_{ramp}-induced V_{hys}, suggesting that the voltage sensitivity of gating charge movements is dependent on the previous state (or conformation) of the

K_M channel. In other words, as the membrane potential becomes depolarized (i.e., during initiation of action potential or the upsloping limb of the triangular V_{ramp}), the voltage dependence of $I_{K(M)}$ activation would switch to less depolarized voltages with a small current magnitude, thereby have the tendency to decrease cell excitability. However, as the membrane potential becomes negative (i.e., downward ramp of the double V_{ramp}), the voltage dependence of K_M channels may shift the mode of V_{hys} to one which occurs at more negative potentials, thereby leading to an increase in membrane repolarization. Furthermore, upon triangular V_{ramp} with varying durations, the QO-58 addition noticeably increased the V_{hys}'s strength for $I_{K(M)}$ elicitation. Under this scenario, we extended previous results and further provided the experimental observations, strongly indicating that there would be a perturbing stimulatory effect of QO-58 on such non-equilibrium property (i.e., V_{hys}) in K_M (or K_V7) channels in electrically excitable cells. However, how QO-58-induced changes in $I_{K(M)}$'s V_{hys} are linked to the behavior of these cells occurring in vivo remains unclear. Of importance, the main point raised is that the adjustments by QO-58 of $I_{K(M)}$'s V_{hys} residing in excitable cells are anticipated to be responsible for altering the bursting pattern of action potentials in excitable cells [13–17,19,20,30,60].

In the present observations, effective EC_{50} value needed for QO-58-stimulated $I_{K(Ca)}$ present in GH_3 cells was yielded to be 4.2 μM, a value that is close to that (3.1 μM) for its activation of $I_{K(M)}$. Under our inside-out current recordings, the addition of QO-58 to bath medium was able to increase the probability of BK_{Ca}-channel openings with being void of change in single-channel conductance, suggesting that QO-58 may bind to a site located on the cytoplasmic leaflet of the α-subunit of BK_{Ca} channels. The slow component of mean closed time of the channel decreased by adding this compound. Under its exposure, the steady-state activation curve of BK_{Ca} channels seen in GH_3 cells became overly shifted to less depolarized potential with no appreciable change in the gating charge of the curve. The QO-58-stimulated BK_{Ca} channel activity was also effectively counteracted by subsequent addition of verruculogen (1 μM), yet not by linopirdine (10 μM). Verruculogen is known to block BK_{Ca} channels effectively [58,59], while linopirdine can suppress K_M-channel activity [18,31,33]. Under such scenario, it is plausible to notice that apart from its effects on $I_{K(M)}$, QO-58-stimulated $I_{K(Ca)}$ arises primarily through the observed activation of BK_{Ca} channels, although the precise or detailed ionic mechanism of QO-58 actions on the activity and gating kinetics of BK_{Ca} channels remains to be resolved.

According to previous pharmacokinetic studies, peak plasma concentration after the oral administration with QO58-lysine with a dose of 50, 20, 12.5 mg/kg has been reported to reach around 50 μg/mL (85 μM), 20 μg/mL (34 μM), or 4 μg/mL (6.8 μM), respectively [5,7]. Moreover, the sensitivity of voltage-clamped cells (e.g., neuroendocrine or endocrine cells) to QO-58 or other structurally similar compounds (e.g., QO-40) can be expected to depend not only on the QO-58 concentration applied, but also greatly on different confounding variables which include the pre-existing level of resting potential and varying bursting patterns of action potential firing. It is therefore conceivable to reflect that QO-58-mediated concerted stimulation of K_M (KCNQx or K_V7x) and BK_{Ca} channels seen in GH_3 cells is of pharmacological or therapeutic relevance, presuming that similar in vivo observations are found [3,8].

4. Materials and Methods

4.1. Chemicals and Solution in This Work

QO-58 (5-(2,6-dichloro-5-fluoropyridin-3-yl)-3-phenyl-2-(trifluoromethyl)-1H-pyrazol-ol[1,5-a]pyrimidin-7-one, 5-(2,6-dichloro-5-fluoro-3-pyridinyl)-3-phenyl-2-(trifluoromethyl)-pyrazolo[1,5-a]pyrimidin-7(4*H*)-one, $C_{18}H_8Cl_2F_4N_4O$) was supplied by Tocris (Union Biomed, Taipei, Taiwan), iberiotoxin and verruculogen (Ver) were by Alomone (Asia Bioscience, Taipei, Taiwan), while we acquired linopirdine, tetrodotoxin (TTX), and thyrotropin releasing hormone (TRH) from Sigma-Aldrich (Merck, Taipei, Taiwan). The stock solution of QO-58 was kept under −20 °C for long-term storage. Unless stated elsewhere, we obtained culture media (e.g., Ham's F-12 medium), horse serum, fetal calf serum,

L-glutamine, and trypsin/EDTA from HyClone™ (Thermo Fisher, Tainan, Taiwan), and other chemicals such as $CdCl_2$, aspartic acid, EGTA, and HEPES were of reagent grade.

The ion composition of extracellular solution (i.e., HEPES-buffered normal Tyrode's solution) that we used in this work was as follows (in mM): NaCl 136.5, KCl 5.4, $CaCl_2$ 1.8, $MgCl_2$ 0.53, glucose 5.5, and HEPES-NaOH buffer 5 (pH 7.4). To record ionic flowing through macroscopic $I_{K(Ca)}$, $I_{K(M)}$ or $I_{K(erg)}$, the patch electrodes were backfilled with the following intracellular solution (in mM): K-aspartate 130, KCl 20, $MgCl_2$ 1, KH_2PO_4 1, Na_2ATP 3, Na_2GTP 0.1, EGTA 0.1, and HEPES-KOH buffer 5 (pH 7.2). To measure $I_{K(M)}$ or $I_{K(erg)}$, we used a high-K^+-bathing solution containing the following (in mM): KCl 145, $MgCl_2$ 0.53, and HEPES-KOH 5 (pH 7.4). To record the activity of single K_M channels, the pipette solution was composed of the following (in mM): NaCl 136.5, KCl 5.4, $MgCl_2$ 0.53, and HEPES-NaOH buffer 5 (pH 7.4), while to measure single BK_{Ca}-channel activity, the pipette solution contained the following (in mM): KCl 145, $MgCl_2$ 0.53, and HEPES-KOH 5 (pH 7.4). All solutions used in this work were prepared in deionized water from a Milli-Q® water purification system (Merck Millipore, Taipei, Taiwan). For the purpose of being sterilized, we filtered the pipette solution and culture media with Acrodisc® syringe filter which contains 0.2-μm Supor® nylon membrane (#4612; Pall Corporation; Genechain, Kaohsiung, Taiwan).

4.2. Cell Preparations

The GH_3 pituitary cell line, which was originally established from a pituitary tumor carried in a 7-month-old female Wistar-Furth rat, was supplied by the Bioresource Collection and Research Center (BCRC-60015; Hsinchu, Taiwan). This cell line was derived from the American Type Culture Collection (ATCC® [CCL-82.1™]; Manassas, VA, USA). We maintained GH_3 cells in Ham's F-12 medium supplemented with 2.5% heat-inactivated fetal calf serum (v/v), 15% horse serum (v/v) and 2 mM L-glutamine [62,64]. Cells were grown in monolayer culture at 37 °C in a humidified environment of CO_2/air (1:19). For sub-culturing made by trypsinization (0.025% trypsin solution [HyClone™] containing 0.01 sodium N,N-diethyldithiocarbamade and EDTA), we dissociated cells and then passaged them every 2–3 days. The measurements were undertaken when cell growth underwent 60–80% confluence (usually 5–6 days).

4.3. Electrophysiological Measurements

Shortly before the experiments, we carefully dissociated cells with a 1% trypsin/EDTA solution, and an aliquot of the suspension containing cell clumps was rapidly placed in a recording chamber adherently attached to the working stage of a DM-IL inverted microscope (Leica; Highrise Instrument, Taichung, Taiwan). The electrodes which were used to record were fabricated from Kimax-51® capillaries with 1.5–1.8 mm in diameter (Kimble® 34500-99; Merck, Taipei, Taiwan) by using a PC-10 vertical puller (Narishige; Taiwan Instrument, Tainan, Taiwan), and their tips were then fire-polished with MF-83 microforge (Narishige). When the electrodes were filled up with different internal solutions described above, their resistance was measured to range between 3 and 5 MΩ, for the purpose of making good GΩ-seal formation. We performed patch clamp recordings in cell-attached, inside-out or whole-cell configuration by using either an RK-400 (Bio-Logic, Claix, France) or an Axopatch-200B amplifier (Molecular Devices; Bestgen Biotech, New Taipei City, Taiwan), as elaborated elsewhere [29,31,52,59]. Whole-cell current recordings were established by rupturing the patch of membrane isolated with GW sealing by the patch pipette, then bringing the cell interior into contact with the pipette interior.

4.4. Data Recordings and Analyses

The signals were monitored and stored online in a Sony VAIO CS series laptop computer (VGN-CS110E; Tainan, Taiwan), equipped with a low-noise 1440A digitizer (Molecular Devices). During the measurements with analog-to-digital and digital-to-analog

conversion, the latter device was controlled by pCLAMP 10.6 software (Molecular Devices) run under Microsoft Windows 7 (Redmond, WA, USA).

To assess the percentage increase of QO-58 on $I_{K(M)}$ or $I_{K(Ca)}$, we measured the amplitudes of $I_{K(M)}$ or $I_{K(Ca)}$ during cell exposure to different QO-58 concentrations (1–300 μM). The amplitude of $I_{K(M)}$ or $I_{K(Ca)}$ during cell exposure to QO-58 at a concentration of 300 μM was considered to be 100%, and the current amplitudes after application of different QO-58 concentrations were expressed relative to this value. The data sets with respect to concentration-dependent effect of QO-58 on the activation of $I_{K(M)}$ or $I_{K(Ca)}$ were satisfactorily fitted to the Hill equation with a nonlinear least-squares' algorithm. Thus:

$$percentage\ increase\ (\%) = \frac{(E_{max} \times [C]^{n_H})}{(EC_{50}^{n_H} + [C]^{n_H})}$$

where [C] = the QO-58 concentration applied; EC_{50} = the QO-58 concentration required for a 50% stimulation; n_H = the Hill coefficient; and E_{max} = the QO-58-induced maximal stimulation of $I_{K(M)}$ or $I_{K(Ca)}$.

The steady-state activation curve (i.e., the relationship of the membrane potential versus the $I_{K(M)}$ conductance) acquired with or without exposure to QO-58 was satisfactorily approximated by a modified Boltzmann function of the following form:

$$\frac{G}{G_{max}} = \frac{1}{\{1 + exp[-(V - V_{1/2})qF/RT]\}}$$

where G = the $I_{K(M)}$ conductance; G_{max} = the maximal conductance of $I_{K(M)}$; $V_{1/2}$ = the voltage at which half-maximal activation of the current is achieved; q = the apparent gating charge; F = Faraday's constant; R = the universal gas constant; and T = the absolute temperature.

The sigmoidal relationship between the membrane potentials and relative open-state probability of BK_{Ca} channels (i.e., the steady-state activation curve) with or without the QO-58 (3 μM) addition was collated and thereafter fitted by the Boltzmann equation using the goodness-of-fitness test;

$$\text{relative open probability} = \frac{n}{\{1 + exp[-(V - V_{1/2})qF/RT]\}} \quad (1)$$

where n = the maximal relative open probability; V = the membrane potential; $V_{1/2}$ = the potential for half-maximal activation; q = apparent gating charge; and F, R, and T are similarly stated above in the activation curve of $I_{K(M)}$.

4.5. Curve-Fitting Approximations and Statistical Analyses

Linear (e.g., single-channel conductance) or nonlinear (e.g., Hill or Boltzmann equation and single exponential) curves fitted to different experimental data sets were made with chi-squared goodness-of-fit test using either the Solver add-in bundled with Excel® 2021 (Microsoft, Redmond, WA, USA)) or OriginPro® 2021 (OriginLab, Scientific Formosa, Kaohsiung, Taiwan). The values are provided as means ± error of the mean (SEM) with the sizes of experimental observations, which represent the cell number sampled. The Student's t-test (paired or unpaired) for two different group, or analyses of variance (ANOVA-1 or ANOVA-2) followed by post-hoc Fisher's least-significance difference among more than two different groups studied for multiple comparisons, were made for the statistical evaluation. Probability with $p < 0.05$ was considered statistically significant (as indicated with * or ** in the figures), unless noted otherwise.

Author Contributions: Conceptualization, S.-N.W., C.-L.W., P.F., H.-Y.C. and T.-H.C.; methodology, S.-N.W.; software, S.-N.W.; validation, C.-L.W., P.F., H.-Y.C., T.-H.C. and S.-N.W.; formal analysis, S.-N.W.; investigation, H.-Y.C., T.-H.C. and S.-N.W.; resources, S.-N.W.; data curation, S.-N.W.; writing—original draft preparation, S.-N.W.; writing—review and editing, C.-L.W., P.F., H.-Y.C., T.-H.C. and S.-N.W.; visualization, H.-Y.C., T.-H.C. and S.-N.W.; supervision, C.-L.W., P.F. and S.-N.W.; project administration, C.-L.W., P.F. and S.-N.W.; funding acquisition, C.-L.W., P.F. and S.-N.W. All authors have read and agreed to the published version of the manuscript.

Funding: The research was partly supported by a grant awarded by Ministry of Science and Technology, Taiwan (MOST-110-2320-B-006-028) to S.-N.W.; Ditmanson Medical Foundation Chia-Yi Christian Hospital. The funders in this work are not involved in the study, design, data collection, analyses, or interpretation.

Institutional Review Board Statement: Not applicable.

Informed Consent Statement: Not applicable.

Data Availability Statement: The original data is available upon reasonable request to the corresponding author.

Acknowledgments: The authors gratefully acknowledge to Meng-Cheng Yu for his assistance in cell preparations.

Conflicts of Interest: The authors declare no conflict of interests that are directly relevant to the present study. The content and writing of this paper are solely the responsibility of the authors.

Abbreviations

BK_{Ca} channel	large-conductance Ca^{2+}-activated K^+ channel
EC_{50}	concentration required for 50% stimulation
I-V	current versus voltage
$I_{K(Ca)}$	Ca^{2+}-activated K^+ current
$I_{K(erg)}$	*erg*-mediated K^+ current
$I_{K(M)}$	M-type K^+ current
K_M channel	M-type K^+ channel
QO-58	5-(2,6-dichloro-5-fluoropyridin-3-yl)-3-phenyl-2-(trifluoromethyl)-1H-pyrazolol[1,5-a]pyrimidin-7-one/5-(2,6-dichloro-5-fluoro-3-pyridinyl)-3-phenyl-2-(trifluoromethyl)-pyrazolo[1,5-a]pyrimidin-7(4*H*)-one)
SEM	standard error of the mean
TRH	thyrotropin releasing hormone
TTX	tetrodotoxin
τ_{act}	activation time constant
V_{hys}	voltage-dependent hysteresis
V_{ramp}	ramp voltage

References

1. Qi, J.; Zhang, F.; Mi, Y.; Fu, Y.; Xu, W.; Zhang, D.; Wu, Y.; Du, X.; Jia, Q.; Wang, K.; et al. Design, synthesis and biological activity of pyrazolo[1,5-a]pyrimidin-7(4H)-ones as novel Kv7/KCNQ potassium channel activators. *Eur. J. Med. Chem.* **2011**, *46*, 934–943. [CrossRef]
2. Zhang, F.; Mi, Y.; Qi, J.L.; Li, J.W.; Si, M.; Guan, B.C.; Du, X.N.; An, H.L.; Zhang, H.L. Modulation of K(v)7 potassium channels by a novel opener pyrazolo[1,5-a]pyrimidin-7(4H)-one compound QO-58. *Br. J. Pharmacol.* **2013**, *168*, 1030–1042. [CrossRef] [PubMed]
3. Zhang, J.; Jia, Q.; Qi, J.; Zhang, H.; Wu, Y.; Shi, X. Exploring in vivo metabolism and excretion of QO-58L using ultra-high-performance liquid chromatography coupled with tandem mass spectrometry. *Eur. J. Pharm. Sci.* **2018**, *117*, 379–391. [CrossRef]
4. Zhang, F.; Liu, Y.; Zhang, D.; Fan, X.; Shao, D.; Li, H. Suppression of KCNQ/M Potassium Channel in Dorsal Root Ganglia Neurons Contributes to the Development of Osteoarthritic Pain. *Pharmacology* **2019**, *103*, 257–262. [CrossRef]
5. Teng, B.-C.; Song, Y.; Zhang, F.; Ma, T.-Y.; Qi, J.-L.; Zhang, H.-L.; Li, G.; Wang, K. Activation of neuronal Kv7/KCNQ/M-channels by the opener QO58-lysine and its anti-nociceptive effects on inflammatory pain in rodents. *Acta Pharmacol. Sin.* **2016**, *37*, 1054–1062. [CrossRef]
6. Du, M.Z.; Duan, R.; Shao, D.C.; Zhang, X.Y.; Zhang, F.; Li, H. Antinociceptive efficacy of QO-58 in the monosodium lodoacetate rat model for osteoarthritis pain. *Zhonghua Yi Xue Za Zhi* **2017**, *97*, 1333–1336.

7. Liu, C.-F.; Qi, J.; Zhang, H.-L.; Jia, Q.-Z. Pharmacokinetic study of QO-58: A new potassium channel opener. *Chin. Pharmacol. Bull.* **2014**, *30*, 574–577.
8. Sheng, Z.-F.; Zhang, H.; Zheng, P.; Chen, S.; Gu, Z.; Zhou, J.-J.; Phaup, J.G.; Chang, H.-M.; Yeh, E.T.H.; Pan, H.-L.; et al. Impaired Kv7 channel activity in the central amygdala contributes to elevated sympathetic outflow in hypertension. *Cardiovasc. Res.* **2022**, *118*, 585–596. [CrossRef]
9. Chang, W.T.; Wu, S.N. Effective Activation of BK(Ca) Channels by QO-40 (5-(Chloromethyl)-3-(Naphthalen-1-yl)-2-(Trifluoromethyl)Pyrazolo [1,5-a]pyrimidin-7(4H)-one), Known to Be an Opener of KCNQ2/Q3 Channels. *Pharmaceuticals* **2021**, *14*, 388. [CrossRef]
10. Wang, H.-S.; Pan, Z.; Shi, W.; Brown, B.S.; Wymore, R.S.; Cohen, I.S.; Dixon, J.E.; McKinnon, D. KCNQ2 and KCNQ3 potassium channel subunits: Molecular correlates of the M-channel. *Science* **1998**, *282*, 1890–1893. [CrossRef] [PubMed]
11. Gribkoff, V.K. The therapeutic potential of neuronal KCNQ channel modulators. *Expert Opin. Ther. Targets* **2003**, *7*, 737–748. [CrossRef]
12. Wulfsen, I.; Hauber, H.P.; Schiemann, D.; Bauer, C.K.; Schwarz, J.R. Expression of mRNA for voltage-dependent and inward-rectifying K channels in GH_3/B_6 cells and rat pituitary. *J. Neuroendocrinol.* **2000**, *12*, 263–272. [CrossRef]
13. Yue, C.; Yaari, Y. KCNQ/M channels control spike afterdepolarization and burst generation in hippocampal neurons. *J. Neurosci.* **2004**, *24*, 4614–4624. [CrossRef]
14. Hernández, C.C.; Zaika, O.; Tolstykh, G.P.; Shapiro, M.S. Regulation of neural KCNQ channels: Signalling pathways, structural motifs and functional implications. *J. Physiol.* **2008**, *586*, 1811–1821. [CrossRef]
15. Brown, D.A.; Passmore, G.M. Neural KCNQ (Kv7) channels. *Br. J. Pharmacol.* **2009**, *156*, 1185–1195. [CrossRef]
16. Greene, D.L.; Hoshi, N. Modulation of Kv7 channels and excitability in the brain. *Cell Mol. Life Sci.* **2017**, *74*, 495–508. [CrossRef]
17. Hu, B.; Cilz, N.I.; Lei, S. Somatostatin depresses the excitability of subicular bursting cells: Roles of inward rectifier K^+ channels, KCNQ channels and Epac. *Hippocampus* **2017**, *27*, 971–984. [CrossRef]
18. Li, T.; Wu, K.; Yue, Z.; Wang, Y.; Zhang, F.; Shen, H. Structural Basis for the Modulation of Human KCNQ4 by Small-Molecule Drugs. *Mol. Cell* **2021**, *81*, 25–37.e4. [CrossRef]
19. Ramakrishna, Y.; Manca, M.; Glowatzki, E.; Sadeghi, S.G. Cholinergic Modulation of Membrane Properties of Calyx Terminals in the Vestibular Periphery. *Neuroscience* **2021**, *452*, 98–110. [CrossRef]
20. Revill, A.L.; Katzell, A.; Del Negro, C.A.; Milsom, W.K.; Funk, G.D. KCNQ Current Contributes to Inspiratory Burst Termination in the Pre-Bötzinger Complex of Neonatal Rats in vitro. *Front. Physiol.* **2021**, *12*, 626470. [CrossRef]
21. Wua, Y.J.; Dworetzky, S.I. Recent developments on KCNQ potassium channel openers. *Curr. Med. Chem.* **2005**, *12*, 453–460. [CrossRef]
22. Munro, G.; Dalby-Brown, W. Kv7 (KCNQ) channel modulators and neuropathic pain. *J. Med. Chem.* **2007**, *50*, 2576–2582. [CrossRef]
23. Sun, J.; Kapur, J. M-type potassium channels modulate Schaffer collateral-CA1 glutamatergic synaptic transmission. *J. Physiol.* **2012**, *590*, 3953–3964. [CrossRef]
24. Allen, N.M.; Mannion, M.; Conroy, J.; Lynch, S.A.; Shahwan, A.; Lynch, B.; King, M.D. The variable phenotypes of KCNQ-related epilepsy. *Epilepsia* **2014**, *55*, e99–e105. [CrossRef]
25. Wang, J.-J.; Li, Y. KCNQ potassium channels in sensory system and neural circuits. *Acta Pharmacol. Sin.* **2015**, *37*, 25–33. [CrossRef]
26. Barrese, V.; Stott, J.B.; Greenwood, I.A. KCNQ-Encoded Potassium Channels as Therapeutic Targets. *Annu. Rev. Pharmacol. Toxicol.* **2018**, *58*, 625–648. [CrossRef]
27. Vanhoof-Villalba, S.L.; Gautier, N.M.; Mishra, V.; Glasscock, E. Pharmacogenetics of KCNQ channel activation in 2 potassium channelopathy mouse models of epilepsy. *Epilepsia* **2017**, *59*, 358–368. [CrossRef]
28. Lezmy, J.; Gelman, H.; Katsenelson, M.; Styr, B.; Tikochinsky, E.; Lipinsky, M.; Peretz, A.; Slutsky, I.; Attali, B. M-Current Inhibition in Hippocampal Excitatory Neurons Triggers Intrinsic and Synaptic Homeostatic Responses at Different Temporal Scales. *J. Neurosci.* **2020**, *40*, 3694–3706. [CrossRef]
29. Cho, H.Y.; Chuang, T.H.; Wu, S.N. The Effectiveness in Activating M-Type K^+ Current Produced by Solifenacin ([(3R)-1-azabicyclo[2.2.2]octan-3-yl] (1S)-1-phenyl-3,4-dihydro-1H-isoquinoline-2-carboxylate): Independent of Its Antimuscarinic Action. *Int. J. Mol. Sci.* **2021**, *22*, 12399. [CrossRef]
30. Jones, F.; Gamper, N.; Gao, H. Kv7 Channels and Excitability Disorders. In *Handbook of Experimental Pharmacology*; Springer: Berlin/Heidelberg, Germany, 2021; pp. 185–230.
31. Lo, Y.-C.; Lin, C.-L.; Fang, W.-Y.; Lőrinczi, B.; Szatmári, I.; Chang, W.-H.; Fülöp, F.; Wu, S.-N. Effective Activation by Kynurenic Acid and Its Aminoalkylated Derivatives on M-Type K^+ Current. *Int. J. Mol. Sci.* **2021**, *22*, 1300. [CrossRef]
32. Costi, S.; Han, M.-H.; Murrough, J.W. The Potential of KCNQ Potassium Channel Openers as Novel Antidepressants. *CNS Drugs* **2022**, *36*, 207–216. [CrossRef]
33. Flunker, L.; Nutter, T.; Bowers, C.; Cooper, B. Development of KVO treatment strategies for chronic pain in a rat model of Gulf War Illness. *Toxicol. Appl. Pharmacol.* **2021**, *434*, 115821. [CrossRef]
34. Li, S.-B.; Damonte, V.M.; Chen, C.; Wang, G.X.; Kebschull, J.M.; Yamaguchi, H.; Bian, W.-J.; Purmann, C.; Pattni, R.; Urban, A.E.; et al. Hyperexcitable arousal circuits drive sleep instability during aging. *Science* **2022**, *375*, eabh3021. [CrossRef]
35. Osuma, A.T.; Xu, X.; Wang, Z.; Van Camp, J.A.; Freiberg, G.M. Design and evaluation of pyrazolopyrimidines as KCNQ channel modulators. *Bioorganic Med. Chem. Lett.* **2019**, *29*, 126603. [CrossRef]

36. Redford, K.E.; Abbott, G.W. KCNQ Potassium Channels as Targets of Botanical Folk Medicines. *Annu. Rev. Pharmacol. Toxicol.* **2022**, *62*, 447–464. [CrossRef]
37. Selyanko, A.A.; Hadley, J.K.; Wood, I.C.; Abogadie, F.C.; Delmas, P.; Buckley, N.J.; London, B.; Brown, D.A. Two Types of K^+ Channel Subunit, Erg1 and KCNQ2/3, Contribute to the M-Like Current in a Mammalian Neuronal Cell. *J. Neurosci.* **1999**, *19*, 7742–7756. [CrossRef]
38. Hsiao, H.T.; Liu, Y.C.; Liu, P.Y.; Wu, S.N. Concerted suppression of I(h) and activation of I(K(M)) by ivabradine, an HCN-channel inhibitor, in pituitary cells and hippocampal neurons. *Brain Res. Bull.* **2019**, *149*, 11–20. [CrossRef]
39. So, E.C.; Liu, P.Y.; Wu, S.N. Effectiveness in the inhibition of dapagliflozin and canagliflozin on M-type K^+ current and α-methylglucoside-induced current in pituitary tumor (GH_3) and pheochromocytoma PC12 cells. *Eur. J. Pharmacol.* **2020**, *879*, 173141. [CrossRef]
40. Kis, A.; Krick, S.; Baumlin, N.; Salathe, M. Airway Hydration, Apical K^+ Secretion, and the Large-Conductance, Ca^{2+}-activated and Voltage-dependent Potassium (BK) Channel. *Ann. Am. Thorac. Soc.* **2016**, *13*, S163–S168.
41. Barkai, O.; Goldstein, R.H.; Caspi, Y.; Katz, B.; Lev, S.; Binshtok, A.M. The Role of Kv7/M Potassium Channels in Controlling Ectopic Firing in Nociceptors. *Front. Mol. Neurosci.* **2017**, *10*, 181. [CrossRef]
42. Latorre, R.; Castillo, K.; Carrasquel-Ursulaez, W.; Sepulveda, R.V.; Gonzalez-Nilo, F.; Gonzalez, C.; Alvarez, O. Molecular Determinants of BK Channel Functional Diversity and Functioning. *Physiol. Rev.* **2017**, *97*, 39–87. [CrossRef] [PubMed]
43. Al-Karagholi, M.A.; Gram, C.; Nielsen, C.A.W.; Ashina, M. Targeting BK(Ca) Channels in Migraine: Rationale and Perspectives. *CNS Drugs* **2020**, *34*, 325–335. [CrossRef] [PubMed]
44. Lu, T.L.; Gao, Z.H.; Li, S.W.; Wu, S.N. High Efficacy by GAL-021: A Known Intravenous Peripheral Chemoreceptor Modulator that Suppresses BK(Ca)-Channel Activity and Inhibits I(K(M)) or I(h). *Biomolecules* **2020**, *10*, 188. [CrossRef] [PubMed]
45. Cui, J. BK Channel Gating Mechanisms: Progresses Toward a Better Understanding of Variants Linked Neurological Diseases. *Front. Physiol.* **2021**, *12*, 762175. [CrossRef]
46. Niday, Z.; Bean, B.P. BK Channel Regulation of Afterpotentials and Burst Firing in Cerebellar Purkinje Neurons. *J. Neurosci.* **2021**, *41*, 2854–2869. [CrossRef] [PubMed]
47. Schrøder, R.L.; Strøbaek, D.; Olesen, S.P.; Christophersen, P. Voltage-independent KCNQ4 currents induced by (+/−)BMS-204352. *Pflug. Arch.* **2003**, *446*, 607–616. [CrossRef] [PubMed]
48. Hsu, H.T.; Tseng, Y.T.; Lo, Y.C.; Wu, S.N. Ability of naringenin, a bioflavonoid, to activate M-type potassium current in motor neuron-like cells and to increase BKCa-channel activity in HEK293T cells transfected with α-hSlo subunit. *BMC Neurosci.* **2014**, *15*, 135. [CrossRef] [PubMed]
49. Sankaranarayanan, S.; Simasko, S. Characterization of an M-like current modulated by thyrotropin-releasing hormone in normal rat lactotrophs. *J. Neurosci.* **1996**, *16*, 1668–1678. [CrossRef]
50. Schwarz, J.R.; Bauer, C.K. Functions of erg K^+ channels in excitable cells. *J. Cell Mol. Med.* **2004**, *8*, 22–30. [CrossRef]
51. Vandenberg, J.I.; Perry, M.D.; Perrin, M.J.; Mann, S.A.; Ke, Y.; Hill, A.P. hERG K^+ channels: Structure, function, and clinical significance. *Physiol. Rev.* **2012**, *92*, 1393–1478. [CrossRef]
52. So, E.C.; Foo, N.P.; Ko, S.Y.; Wu, S.N. Bisoprolol, Known to Be a Selective β_1-Receptor Antagonist, Differentially but Directly Suppresses $I_{K(M)}$ and $I_{K(erg)}$ in Pituitary Cells and Hippocampal Neurons. *Int. J. Mol. Sci.* **2019**, *20*, 657. [CrossRef]
53. Männikkö, R.; Pandey, S.; Larsson, H.P.; Elinder, F. Hysteresis in the voltage dependence of HCN channels: Conversion between two modes affects pacemaker properties. *J. Gen. Physiol.* **2005**, *125*, 305–326. [CrossRef] [PubMed]
54. Fürst, O.; D'Avanzo, N. Isoform dependent regulation of human HCN channels by cholesterol. *Sci. Rep.* **2015**, *5*, 14270. [CrossRef] [PubMed]
55. Selyanko, A.; Brown, D. Regulation of M-type Potassium Channels in Mammalian Sympathetic Neurons: Action of Intracellular Calcium on Single Channel Currents. *Neuropharmacology* **1996**, *35*, 933–947. [CrossRef]
56. Wu, S.N.; Lo, Y.K.; Li, H.F.; Shen, A.Y. Functional coupling of voltage-dependent L-type Ca^{2+} current to Ca^{2+}-activated K^+ current in pituitary GH3 cells. *Chin. J. Physiol.* **2001**, *44*, 161–167. [PubMed]
57. Plante, A.E.; Whitt, J.P.; Meredith, A.L. BK channel activation by L-type Ca^{2+} channels $Ca_V1.2$ and $Ca_V1.3$ during the subthreshold phase of an action potential. *J. Neurophysiol.* **2021**, *126*, 427–439. [CrossRef]
58. Knaus, H.G.; McManus, O.B.; Lee, S.H.; Schmalhofer, W.A.; Garcia-Calvo, M.; Helms, L.M.; Sanchez, M.; Giangiacomo, K.; Reuben, J.P.; Smith, A.B., 3rd; et al. Tremorgenic Indole Alkaloids Potently Inhibit Smooth Muscle High-Conductance Calcium-Activated Potassium Channels. *Biochemistry* **1994**, *33*, 5819–5828. [CrossRef] [PubMed]
59. Wu, S.-N.; Chern, J.-H.; Shen, S.; Chen, H.-H.; Hsu, Y.-T.; Lee, C.-C.; Chan, M.-H.; Lai, M.-C.; Shie, F.-S. Stimulatory actions of a novel thiourea derivative on large-conductance, calcium-activated potassium channels. *J. Cell. Physiol.* **2017**, *232*, 3409–3421. [CrossRef]
60. Zhou, J.-J.; Gao, Y.; Kosten, T.A.; Zhao, Z.; Li, D.-P. Acute stress diminishes M-current contributing to elevated activity of hypothalamic-pituitary-adrenal axis. *Neuropharmacology* **2016**, *114*, 67–76.
61. Bauer, C.K.; Schwarz, J.R. Ether-à-go-go K^+ channels: Effective modulators of neuronal excitability. *J. Physiol.* **2018**, *596*, 769–783. [CrossRef] [PubMed]
62. Bauer, C.K.; Schwarz, J.R. Evidence for the Effectiveness of Remdesivir (GS-5734), a Nucleoside-Analog Antiviral Drug in the Inhibition of $I_{K(M)}$ or $I_{K(DR)}$ and in the Stimulation of I (MEP). *Front. Pharmacol.* **2020**, *11*, 1091.

63. Chen, L.; Cho, H.-Y.; Chuang, T.-H.; Ke, T.-L.; Wu, S.-N. The Effectiveness of Isoplumbagin and Plumbagin in Regulating Amplitude, Gating Kinetics, and Voltage-Dependent Hysteresis of *erg*-mediated K^+ Currents. *Biomedicines* **2022**, *10*, 780. [CrossRef] [PubMed]
64. Hung, T.-Y.; Wu, S.-N.; Huang, C.-W. The Integrated Effects of Brivaracetam, a Selective Analog of Levetiracetam, on Ionic Currents and Neuronal Excitability. *Biomedicines* **2021**, *9*, 369. [CrossRef] [PubMed]